# Supporting Information

Aman et al. 10.1073/pnas.1424435112

## SI Materials and Methods

**Phylogenetic Analysis.** Using the SeaView package (1), we aligned individual 12S rRNA, 16S rRNA, and cytochrome oxidase subunit I (COI) sequences with MUSCLE (2) and then estimated parameters of sequence evolution based on neighbor-joining trees using PhyML (3). Again using PhyML, we inferred maximum-likelihood trees using a GTR+I+G model (4) for individual genes and for the concatenated sequences of all three genes using approximate likelihood ratio test (aLRT) statistics to provide branch length support for the trees. For partitioned maximum-likelihood analyses of the same sequences, we used RAxML (5) to optimize the maximum-likelihood tree using the GTR+G model with parameters estimated separately for each gene. In addition, we used MrBayes (6, 7) to infer model parameters and the consensus tree using optimal GTR+I+G partitioning for the concatenated sequences of all three genes. Each analysis comprised two simultaneous runs with four chains each for enough generations to reduce the average SD of the split frequencies below 0.01 (about 17 million generations). Trees and parameters from the first 25% of the generations were discarded (the burn-in) after completion of the Monte Carlo Markov chain search. Posterior probabilities provide additional branch support for the tree.

**Cloning of 12S and 16S Mitochondrial RNA Segments, the Partial Cytochrome Oxidase Subunit I Mitochondrial RNA Gene Segment, and Intron 9 of the γ-Glutamyl Carboxylase Gene.** Genomic DNA from each specimen was used as a template for PCR with oligonucleotides corresponding to 12S-I/12S-3 mitochondrial rRNA segments (590 bp) (8), 16SH/16LC mitochondrial rRNA segments (548 bp) (9), LCO1490/HCO2198 cytochrome oxidase subunit I gene segments (603 bp) (10), and exons 9/10 of **γ**-glutamyl carboxylase (of which a 259-bp conserved intronic sequence was analyzed) (11). Cloning and sequencing of these products were performed as previously described (11, 12). Sequences were deposited in GenBank (Table S1).

**Status of Vouchers.** Many of the specimens analyzed were originally collected to identify conotoxin genes. These were gathered and prepared long before phylogenetic analysis was considered and long before vouchers were required. Hence, although we do not have a complete set of voucher specimens, there has been no reason to doubt the authenticity of the samples or the validity of the research. Nevertheless, to correct this shortcoming for future studies, we are now systematically replicating this analysis using bar coding and are depositing vouchers of the replicates at the Marine Science Institute at the University of the Philippines.

**Fractionation of Venom Components from *C. tessulatus* and *C. eburneus* Venom Ducts.** Frozen *C. tessulatus* venom ducts from specimens collected near Olango Island, Cebu, Philippines were thawed in 12 mL of 35% (vol/vol) acetonitrile in 0.1% (vol/vol) trifluoroacetic acid (TFA) and cut into small fragments while in solution. Venom-duct fragments were homogenized and centrifuged immediately at 37,500 × *g* (13). The pellet was suspended in 3 mL of the same solution and the mixture was homogenized and centrifuged. The supernatants were combined, processed, and fractionated on a Vydac preparative C18 column (13). The HPLC profile at 220 nm is shown in Fig. 3*A*. Aliquots of fractions and fraction pools were dried in a SpeedVac concentrator for subsequent bioassays. The active HPLC fraction 44 (Fig. 3) was subfractionated on a Vydac analytical monomeric C18 column using a solvent gradient of 0.33% increase per min in the concentration of solvent B [solvent A was 0.1% (vol/vol) TFA; solvent B was 90% (vol/vol) acetonitrile in 0.1% TFA]. The active component eluted at ∼62% solvent B.

Frozen *C. eburneus* ducts, obtained from specimens collected near Olango Island, Cebu, Philippines and Guam Island, were pooled and processed following the procedure used for the *C. tessulatus* venom ducts mentioned above, with the following modifications: 45% (vol/vol) acetonitrile in 0.1% TFA was used to prepare the crude extract, and no further fractionation was needed to obtain a pure sample of the active peptide.

**Bioassay-Guided Purification of δ-Conotoxins TsVIA and ErVIA.** Aliquots of pooled and individual HPLC venom fractions were assayed for activity on dissociated DRG neurons by calcium imaging (Fig. 3 and Fig. S5). The calcium-imaging methods have been described in detail previously (14–17). Briefly, all lumbar DRG were removed from C57BL6 mice and the cells were dissociated by enzymatic and mechanical treatments, after which the cells were cultured overnight. The cells were loaded with Fura-2 AM for 1 h at 37 °C and 30 min at room temperature and then processed for calcium imaging. Each calcium-imaging trace in Figs. 3*B* and 4 *A* and *B* and Fig. S5*B* represents the responses of a single neuron. Upward deflection of a trace represents a transient increase in cytosolic calcium concentration. The *y* axis of calcium-imaging traces is the ratio of fluorescence emission at 510 nm upon alternating excitation at 340 nm and 380 nm (340/380 nm), a relative measure of cytosolic calcium concentration. The experimental protocol shown below the *x* axis of calcium-imaging traces applies to all traces in a panel.

**Mass and Partial Amino Acid Sequence of δ-Conotoxin TsVIA.** The mass of the active subfraction from venom fraction 44 (Fig. 3) was determined by matrix-assisted laser desorption ionization (MALDI) mass spectrometry, which indicated a single component with a mass of 2748.16 Da. An aliquot of the fraction was fully reduced and alkylated as described previously (13), and a partial amino acid sequence (CAAFGSFCGLPGLVD…) was obtained by automated Edman degradation using a Procise 491 Protein Sequencing System (Applied Biosystems) using the pulsed-liquid method.

**Sequencing of δ-Conotoxin TsVIA by MS/MS.** The native and derivatized peptides (for which a partial sequence was determined by Edman degradation) were analyzed on the Orbitrap Elite with high resolution as described previously (13). The peptide sequence was determined manually with a ppm error of <15 ppm for all observed fragment ions and <2 ppm for the intact peptide toxin. An aliquot of the purified peptide was loaded onto a New Objective 360 μm o.d. × 75 μm i.d. column with an 8-μm integrated emitter and packed with 20 cm of HALO C18, 2.7 μm, 90 Å material using the autosampler of an EASY-nLC 1000 (Thermo Scientific). The peptide was eluted from the column directly into an Orbitrap Elite mass spectrometer (Thermo Scientific) using a 30-min gradient from 2 to 50% solvent B (solvent A was 2% acetonitrile in 0.5% acetic acid; solvent B was 90% acetonitrile in 0.5% acetic acid). To obtain the accurate mass of the native peptide, high-resolution full-scan spectra were acquired with a resolution of 240,000 at 400 *m/z*, an automatic gain control (AGC) target of 5e5 with a maximum-ion injection time of 500 ms, a scan range of 400–1,400 *m/z*, and polysiloxane 445 *m/z* as lock mass ion.

For the sequence determination, an aliquot of the purified peptide was incubated for 1 h at room temperature with 25 mM TCEP [Tris·(2-carboxyethyl)phosphine] and 1 μL 2-methylaziridine in 500 mM TEAB (triethylammonium bicarbonate) buffer with 10% (vol/vol) acetonitrile. The mixture was acidified with TFA, and the peptide solution was desalted by adding a slurry of R2 20-μm Poros beads (Life Technologies) in 5% formic acid and 0.2% TFA. The beads were loaded onto equilibrated C18 ZipTips (Millipore) using a microcentrifuge for 30 s at 3,099 × *g*. The Poros beads were rinsed three times with 0.1% TFA followed by further washes with 0.5% acetic acid. The peptide was eluted by the addition of 40% acetonitrile in 0.5% acetic acid followed by the addition of 80% acetonitrile in 0.5% acetic acid. The organic solvent was removed using a SpeedVac concentrator and the sample was reconstituted in 0.5% acetic acid. An aliquot of the derivatized peptide was loaded on a New Objective HALO column as described above and spectra were acquired using the following instrument settings: The full scan was recorded with a resolution of 60,000 at 400 *m/z*, an AGC target value of 5e5 with a maximum-ion injection time of 500 ms, a scan range of 300–1,500 *m/z*, and polysiloxane 445 *m/z* as lock mass ion. Following each full scan, the +5 and +6 charge states of the derivatized peptide were subsequently fragmented using electron transfer dissociation (ETD) and the resulting MS/MS spectra were acquired using following instrument parameters: a resolution of 60,000 at 400 *m/z*, and an AGC target value of 1e5 with a maximum-ion injection time of 800 ms and 4 μscans. The resulting MS/MS spectra were interpreted manually. The recorded mass fits the calculated mass of the manually obtained peptide sequence within 1.5 ppm (Fig. S3).

**Molecular Cloning of δ-Conotoxin Sequences.** Because we obtained only a partial sequence for δ-conotoxin TsVIA by Edman degradation, and MS/MS sequencing cannot differentiate between leucine and isoleucine, we also obtained a cloned sequence for the C-terminal end of the peptide, which allowed us to differentiate between leucine and isoleucine, as shown in Fig. S4. RNA was isolated from *C. tessulatus* venom-duct tissue using NucleoSpin RNA XS column purification (manufacturer's suggested protocol; Clontech Laboratories) followed by cDNA library construction using the Clontech In-Fusion SMARTer PCR Directional cDNA Library Construction Kit, according to the manufacturer's instructions. Reverse-transcription PCR was performed using the Clontech Advantage 2 PCR Kit. Oligonucleotides were designed based on sequence similarities with the *C. eburneus* peptide and other members of the δ-conotoxin family [sense primer: 5′-TGC GCT GC(A,T,C,G) TT(T,C) GGT TCG TT-3′; antisense primer: 5′-GA(G/T) GGG AG(G/T) AGA AGA CAT CA-3′]. PCR amplicons were cloned into the pGEM-T Easy Vector (Promega) and transformed into *Escherichia coli* (DH10B strain). Plasmids were purified using a plasmid DNA extraction kit (Viogene-Biotek) and sequenced at the University of Utah Core Sequencing Facility.

A cloned DNA sequence encoding the predicted amino acid sequence of δ-conotoxin ErVIA (shown in Table 1) was identified from *C. eburneus* genomic DNA as previously described (18). Briefly, genomic DNA from *C. eburneus* was used as a template for PCR with oligonucleotides corresponding to conserved regions of the intron 5′ to the mature peptide sequence and the 3′ UTR sequence of δ-conotoxins. The resulting PCR product was purified using the High Pure PCR Product Purification Kit (Roche Diagnostics) following the manufacturer's suggested protocol. The eluted DNA fragments were annealed to the pNEB206A vector using the USER Friendly Cloning Kit (New England BioLabs) following the manufacturer's suggested protocol. The resulting products were transformed into DH5α competent cells. The nucleic acid sequence of this δ-conotoxin–encoding clone was determined according to the standard protocol for automated sequencing at the Health Sciences Center Core Sequencing Facility, University of Utah. This sequence was deposited into GenBank (accession no. KR013220).

**Oocyte Electrophysiology.** Use of *X. laevis* frogs, which provided oocytes for this study, followed protocols approved by the University of Utah Institutional Animal Care and Use Committee that conform to the National Institutes of Health *Guide for the Care and Use of Laboratory Animals* (19). Preparations of cRNA and the injection of cRNA into oocytes were done as previously described (20). Briefly, a given oocyte was injected with 50 nL mouse $Na_V1.6$ cRNA in distilled water (30 ng) with an equal weight of rat $Na_V\beta1$ cRNA. Oocytes were incubated at 16 °C in ND96 (96 mM NaCl, 2 mM KCl, 1.8 mM $CaCl_2$, 1 mM $MgCl_2$, 5 mM Hepes, pH 7.3) supplemented with penicillin/streptomycin, Septra, and Amikacin for 2 d. Oocytes were voltage-clamped with an OC-725C amplifier (Warner Instruments) using 3 M KCl-filled microelectrodes (<0.5 MΩ resistance). The holding potential ($V_{hold}$) was −80 mV, and inward sodium current ($I_{Na}$) was induced every 20 s with a 50-ms depolarizing step to −10 mV. Current signals were filtered at 2 KHz, digitized at a sampling frequency of 10 KHz, and leak-subtracted by a P/8 protocol using in-house software written in LabVIEW (National Instruments). The recording chamber was a 4-mm-diameter well (30 μL total volume) sunk in the silicone elastomer Sylgard (Dow Corning). Conopeptides were dissolved in ND96, and oocytes were exposed to the conopeptides by applying 3 μL of peptide solution (at 10 times the final concentration) to a static bath with a pipettor and manually stirring the bath for a few seconds by gently aspirating and expelling a few microliters of bath fluid several times with the pipettor. All experiments were done at room temperature.


1. Gouy M, Guindon S, Gascuel O (2010) SeaView version 4: A multiplatform graphical user interface for sequence alignment and phylogenetic tree building. *Mol Biol Evol* 27(2):221–224.
2. Edgar RC (2004) MUSCLE: A multiple sequence alignment method with reduced time and space complexity. *BMC Bioinformatics* 5(5):113.
3. Guindon S, et al. (2010) New algorithms and methods to estimate maximum-likelihood phylogenies: Assessing the performance of PhyML 3.0. *Syst Biol* 59(3):307–321.
4. Tavaré S (1986) Some probabilistic and statistical problems in the analysis of DNA sequences. *Am Math Soc Lect Math Life Sci* 17:57–86.
5. Stamatakis A, Ott M, Ludwig T (2005) RAxML-OMP: An efficient program for phylogenetic inference on SMPs. *Proceedings of the 8th International Conference on Parallel Computing Technologies (PaCT2005)*, Lecture Notes in Computer Science, 3506, ed Malyshkin V (Springer, Berlin), pp 288–302.
6. Huelsenbeck JP, Ronquist F, Nielsen R, Bollback JP (2001) Bayesian inference of phylogeny and its impact on evolutionary biology. *Science* 294(5550):2310–2314.
7. Ronquist F, Huelsenbeck JP (2003) MrBayes 3: Bayesian phylogenetic inference under mixed models. *Bioinformatics* 19(12):1572–1574.
8. Simon C, Franke A, Martin A (1991) The polymerase chain reaction: DNA extraction and amplification. *Molecular Techniques in Taxonomy*, eds Hewitt GM, Johnson AWB, Young JPW (Springer, New York), pp 329–355.
9. Palumbi S (1996) Nucleic acids II: The polymerase chain reaction. *Molecular Systematics*, eds Hillis D, Moritz C, Mable BK (Sinauer, Sunderland, MA), pp 205–247.
10. Folmer O, Black M, Hoeh W, Lutz R, Vrijenhoek R (1994) DNA primers for amplification of mitochondrial cytochrome c oxidase subunit I from diverse metazoan invertebrates. *Mol Mar Biol Biotechnol* 3(5):294–299.
11. Kraus NJ, et al. (2011) Against expectation: A short sequence with high signal elucidates cone snail phylogeny. *Mol Phylogenet Evol* 58(2):383–389.
12. Nam HH, Corneli PS, Watkins M, Olivera B, Bandyopadhyay P (2009) Multiple genes elucidate the evolution of venomous snail-hunting *Conus* species. *Mol Phylogenet Evol* 53(3):645–652.
13. Gajewiak J, et al. (2014) A disulfide tether stabilizes the block of sodium channels by the conotoxin μO§-GVIIJ. *Proc Natl Acad Sci USA* 111(7):2758–2763.
14. Smith NJ, et al. (2013) Comparative functional expression of nAChR subtypes in rodent DRG neurons. *Front Cell Neurosci* 7:225.
15. Teichert RW, Memon T, Aman JW, Olivera BM (2014) Using constellation pharmacology to define comprehensively a somatosensory neuronal subclass. *Proc Natl Acad Sci USA* 111(6):2319–2324.
16. Teichert RW, et al. (2012) Characterization of two neuronal subclasses through constellation pharmacology. *Proc Natl Acad Sci USA* 109(31):12758–12763.
17. Teichert RW, et al. (2012) Functional profiling of neurons through cellular neuropharmacology. *Proc Natl Acad Sci USA* 109(5):1388–1395.

18. Biggs JS, Watkins M, Corneli PS, Olivera BM (2010) Defining a clade by morphological, molecular and toxinological criteria: Distinctive forms related to *Conus praecellens* A. Adams, 1854. *Nautilus (Philadelphia)* 124(1):1–19.
19. National Institutes of Health (2011) *Guide for the Care and Use of Laboratory Animals* (The National Academies Press, Washington, DC), 8th Ed.
20. Zhang MM, et al. (2013) Pharmacological fractionation of tetrodotoxin-sensitive sodium currents in rat dorsal root ganglion neurons by μ-conotoxins. *Br J Pharmacol* 169(1):102–114.

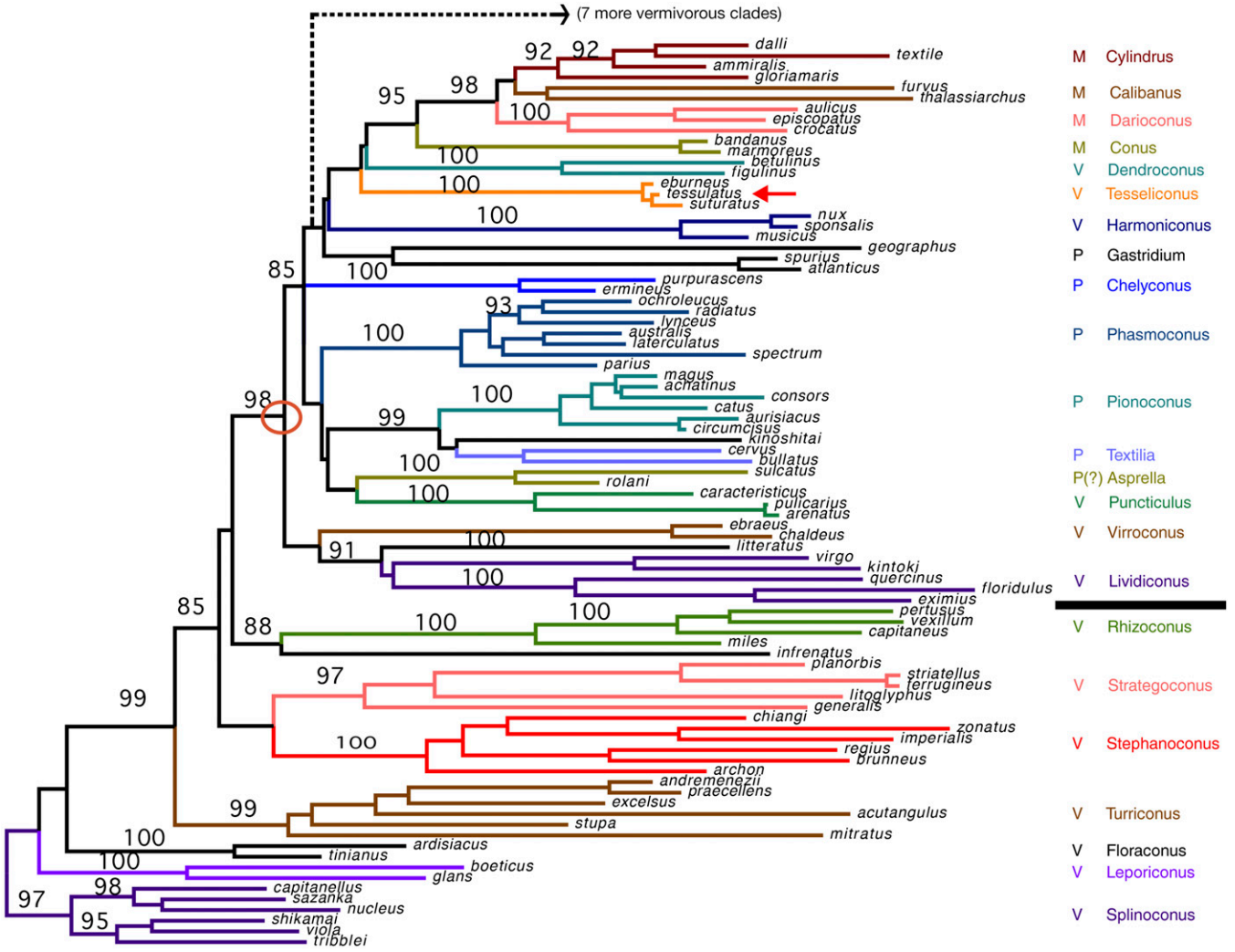


**Fig. S1.** Expanded phylogenetic tree. The tree shown was constructed as described for Fig. 2 of the main text, but 85 species are included. The piscivory of the Asprella clade is inferred but has not been verified by direct observation. There are seven additional vermivorous clades in the major clade A that are indicated but not detailed in the figure (1).

1. Puillandre N, Duda TF, Meyer C, Olivera BM, Bouchet P (2015) One, four or 100 genera? Classification of the cone snails. *J Molluscan Stud* 81(1):1–23.

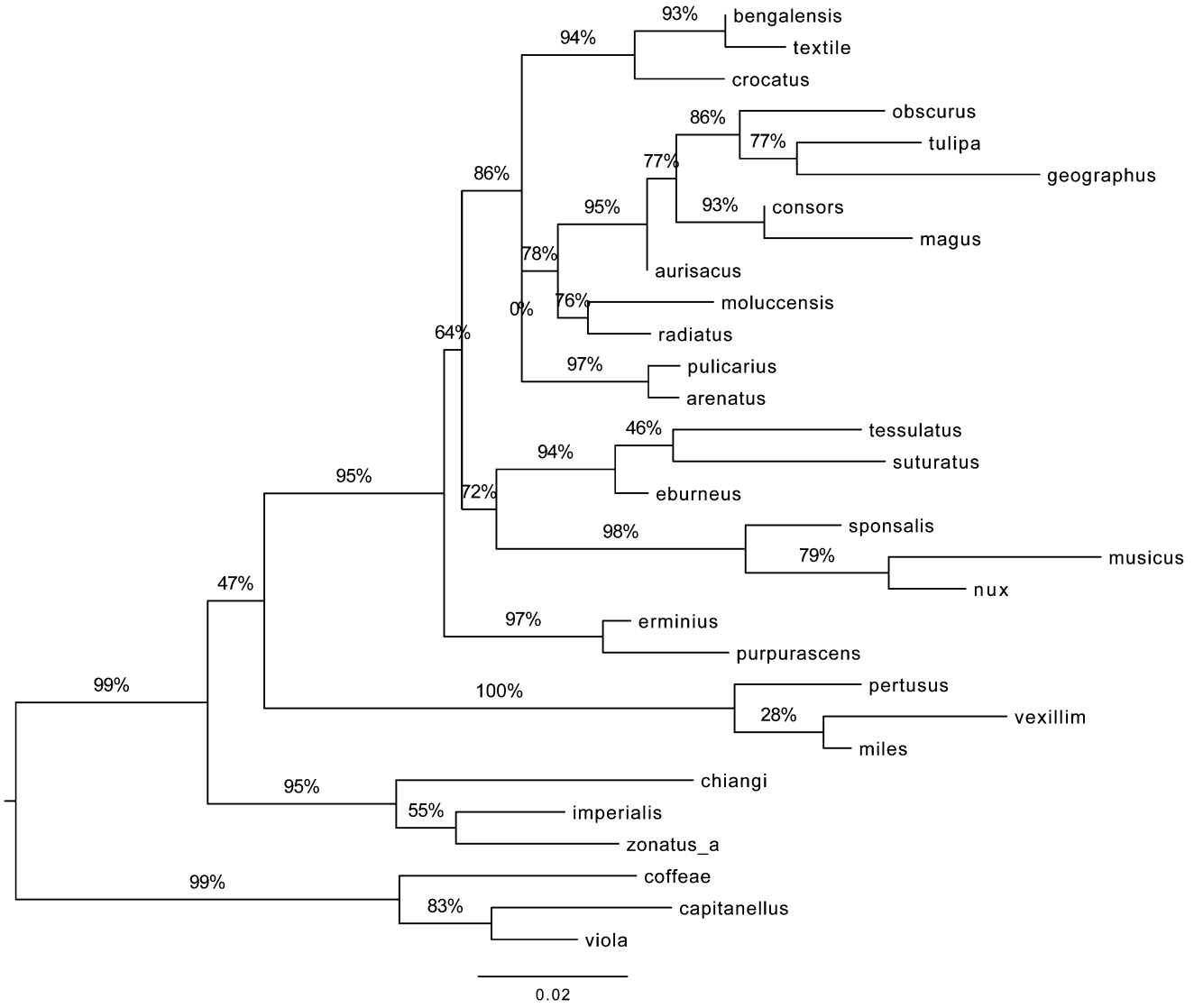


**Fig. S2.** Phylogeny of *C. tessulatus*. Maximum-likelihood tree inferred from a highly informative 282-bp nuclear sequence of intron 9 from the γ-glutamyl carboxylase gene, a posttranslational modification enzyme expressed in *Conus* venom ducts. The tree, although poorly resolved for some clades, has high support (aLRT values) for the placement of *C. tessulatus* nested among the advanced worm-hunting clades.

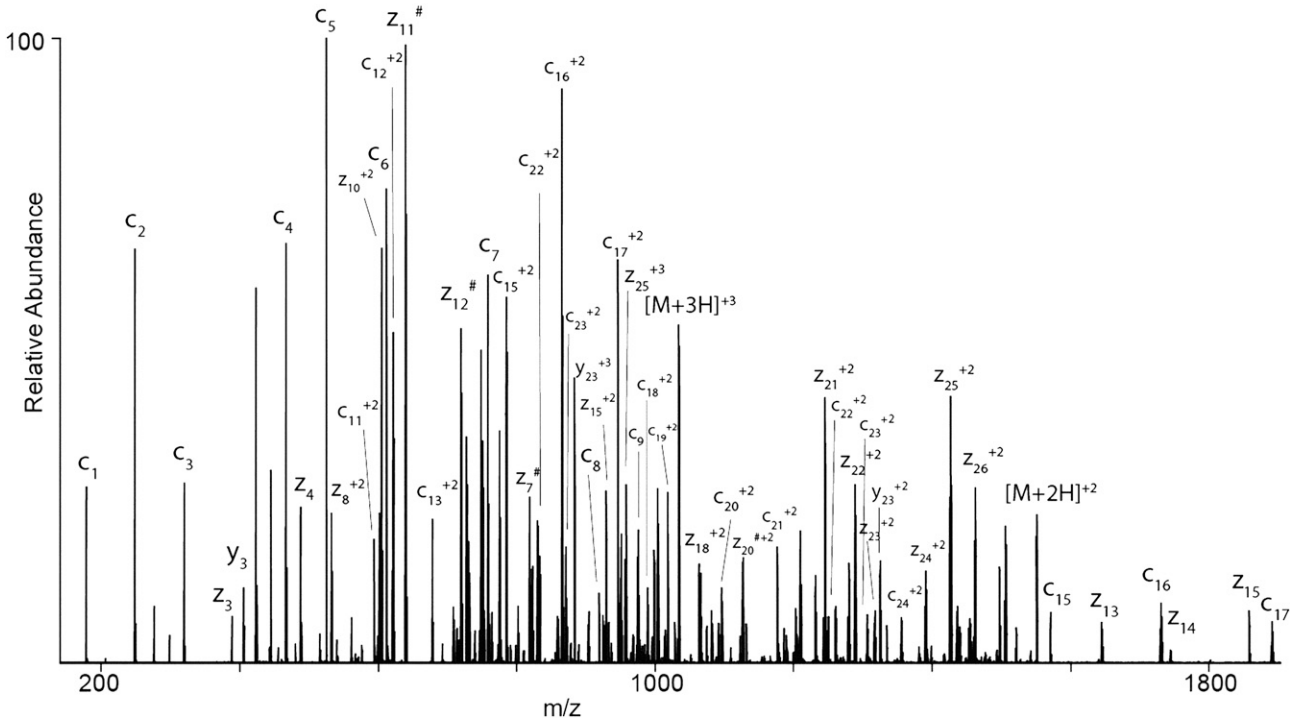


**Fig. S3.** MS/MS ETD spectrum of the $(M+5H)^{+5}$ ion of CAAFGSFCGLPGLVDCCSGRCFIVCLL after reduction and alkylation with 2-methylaziridine acquired on an Orbitrap Elite with 60,000 resolution (at 400 *m/z*). N-terminal fragment ions (C) are indicated by ⌉, and C-terminal fragment ions (Z and Y) are indicated by ⌊. Doubly charged ions are indicated by "+2," and z ions resulting from cleavage at cysteine and loss of the cysteine side chain are indicated by # (1). Due to space limitations, different charge states of already-labeled peptide-bond cleavages are not all indicated in the figure. The mass accuracy for all fragment ions is better than 15 ppm. The mass spectrometer used cannot differentiate between isoleucine or leucine, and the assignment is made here solely with supporting data (i.e., Edman sequencing and homology matching).

1. Chalkley RJ, Brinkworth CS, Burlingame AL (2006) Side-chain fragmentation of alkylated cysteine residues in electron capture dissociation mass spectrometry. *J AmSocMass Spectrom* 17(9):1271–1274.

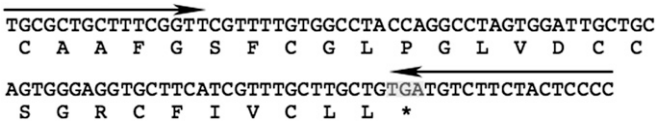


**Fig. S4.** This sequence was obtained by PCR from a *C. tessulatus* cDNA library using primers designed from sequence similarity to the *C. eburneus* peptide, δ-conotoxin ErVIA (Table 1), and other members of the δ-conotoxin family. The locations of the primer sequences are indicated with black arrows. The position of the stop codon is shown (*, highlighted in gray).

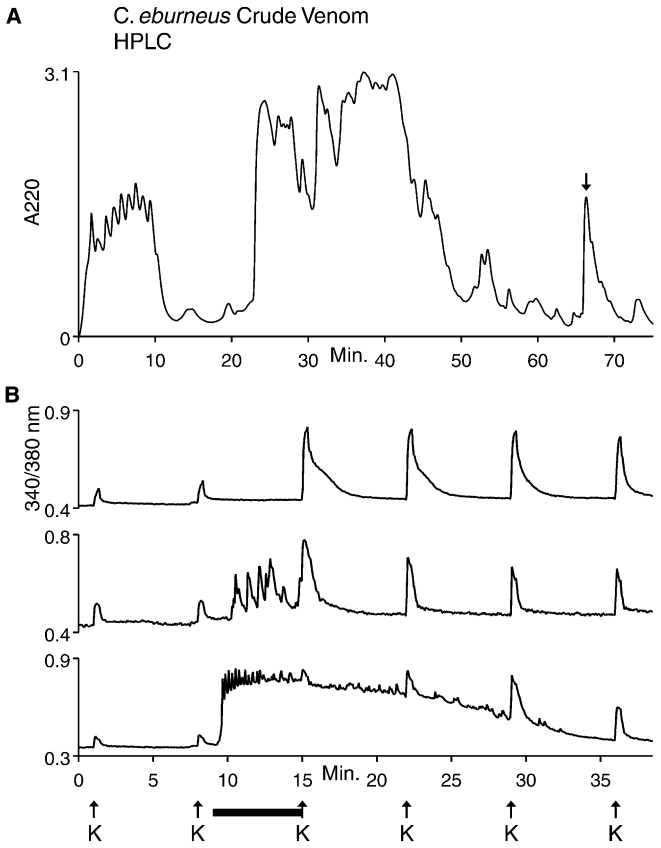


**Fig. S5.** Bioassay-guided purification of δ-conotoxin ErVIA from *C. eburneus* venom. (*A*) Reversed-phase HPLC chromatogram of *C. eburneus* crude venom. The arrow points to the fraction from which δ-conotoxin ErVIA was purified. (*B*) Calcium-imaging traces from selected DRG neurons. Each trace represents the responses of a single neuron. The experimental protocol shown under the *x* axis is as follows. The arrows represent depolarization with 25 mM extracellular potassium. The horizontal bar indicates when the purified δ-conotoxin ErVIA was present in the bath solution. Notably, the activity is the same as that observed from δ-conotoxin TsVIA (Figs. 3 and 4).

**Table S1. GenBank accession numbers for species in Fig. 2 and Fig. S1**

| Species | 12S | 16S | COI | Intron 9 |
|---|---|---|---|---|
| *C. acutangulus* | KJ549690 | KJ549712 | KJ549742 | Not sampled |
| *C. ammiralis* | EU682274 | EU682299 | EU812755 | Not sampled |
| *C. andremenezi* | KJ549691 | KJ549713 | KJ549743 | Not sampled |
| *C. archon* | GU134363 | GU134359 | GU134380 | Not sampled |
| *C. arenatus* | EU781487 | KJ549714 | GU134370 | FJ461229 |
| *C. aurisiacus* | EU682276 | EU078943 | GU134371 | FJ461248 |
| *C. australis* | KJ549692 | KJ549715 | KJ549744 | Not sampled |
| *C. bandanus* | EU682277 | EU794325 | EU733511 | Not sampled |
| *C. bengalensis** | KJ549693 | KJ549716 | Not sampled | KJ549763 |
| *C. capitanellus** | KJ549694 | KJ549717 | KJ549745 | KJ549764 |
| *C. capitaneus* | KJ549695 | KJ549718 | KJ549746 | FJ461238 |
| *C. caracteristicus* | KJ549696 | KJ549719 | KJ549747 | FJ461231 |
| *C. chaldeus* | KJ549697 | KJ549720 | KJ549748 | FJ461234 |
| *C. chiangi* | GU134364 | GU134361 | GU134381 | FJ461240 |
| *C. coffeae** | Not sampled | AF160703 | KJ549749 | KJ549765 |
| *C. consors* | EU682279 | EU078940 | FJ868115 | FJ461247 |
| *C. crocatus** | EU682300 | EU733512 | EU733512 | KJ549766 |
| *C. dalli* | EU682281 | EU078935 | EU733513 | Not sampled |
| *C. ebraeus* | FJ868131 | FJ868146 | KJ549750 | FJ461235 |
| *C. eburneus* | EU682282 | KJ549721 | Not sampled | KJ549767 |
| *C. ermineus* | FJ937336 | FJ937344 | FJ937340 | FJ461245 |
| *C. geographus** | EU794316 | EU794327 | FJ868152 | FJ461249 |
| *C. glans* | FJ868135 | KJ549722 | FJ868159 | Not sampled |
| *C. gloriamaris* | EU733516 | KJ549723 | EU733516 | Not sampled |
| *C. imperialis* | GU134365 | FJ868148 | GU134382 | FJ461239 |
| *C. laterculatus* | EU682287 | EU682287 | GU134372 | Not sampled |
| *C. magus* | EU794319 | EU078939 | FJ868118 | FJ461246 |
| *C. marmoreus* | EU682288 | EU794330 | EU733517 | Not sampled |
| *C. miles** | FJ868130 | KJ549724 | KJ549751 | FJ461236 |
| *C. mitratus* | KJ549698 | KJ549725 | KJ549752 | Not sampled |
| *C. moluccensis** | KJ549699 | KJ549726 | KJ549753 | FJ461242 |
| *C. musicus* | KJ549700 | KJ549727 | KJ549754 | FJ461232 |
| *C. nucleus* | KJ549701 | KJ549728 | KJ549755 | Not sampled |
| *C. nux* | KJ549702 | KJ549729 | Not sampled | KJ549768 |
| *C. obscurus** | EU794321 | EU794331 | KJ549756 | FJ461250 |
| *C. parius* | EU682305 | EU682291 | GU134374 | Not sampled |
| *C. pertusus* | KJ549703 | KJ549730 | KJ549757 | KJ549769 |
| *C. planorbis* | FJ868134 | FJ868149 | FJ868158 | KRO13219 |
| *C. praecellens* | KJ549704 | KJ549731 | Not sampled | Not sampled |
| *C. pulicarius* | EU682292 | KJ549732 | GU134375 | FJ461230 |
| *C. purpurascens* | KJ549705 | KJ549733 | Not sampled | FJ461244 |
| *C. radiatus** | EU682293 | KJ549734 | GU134376 | FJ461241 |
| *C. regius* | GU134368 | AF160725 | GU134385 | Not sampled |
| *C. sponsalis** | KJ549706 | KJ549735 | Not sampled | FJ461233 |
| *C. striatellus* | KJ549707 | KJ549736 | KJ549758 | Not sampled |
| *C. suturatus* | KJ549708 | KJ549737 | Not sampled | KJ606031 |
| *C. tessulatus* | EU682295 | KJ549738 | GU134377 | KJ606032 |
| *C. textile* | EU682296 | EU078936 | EU812758 | AY044904 |
| *C. tribblei* | KJ549709 | KJ549739 | KJ549759 | Not sampled |
| *C. tulipa** | EU794322 | EU794333 | KJ549760 | FJ461251 |
| *C. vexillum* | KJ549710 | KJ549740 | KJ549761 | FJ461237 |
| *C. viola* | KJ549711 | KJ549741 | KJ549762 | KR013218 |
| *C. zonatus* | GU134366 | GU134362 | GU134383 | KJ549770 |

*Species used solely in the intron 9 tree.

**Movie S1.** *Conus tessulatus* engulfing its worm prey. The worm was placed in front of the snail; the recorded feeding sequence is notable in that the snail did not envenomate the worm before engulfing it (in contrast to Fig. 1, *Bottom Right*, showing the snail injecting venom into its prey).

Movie S1

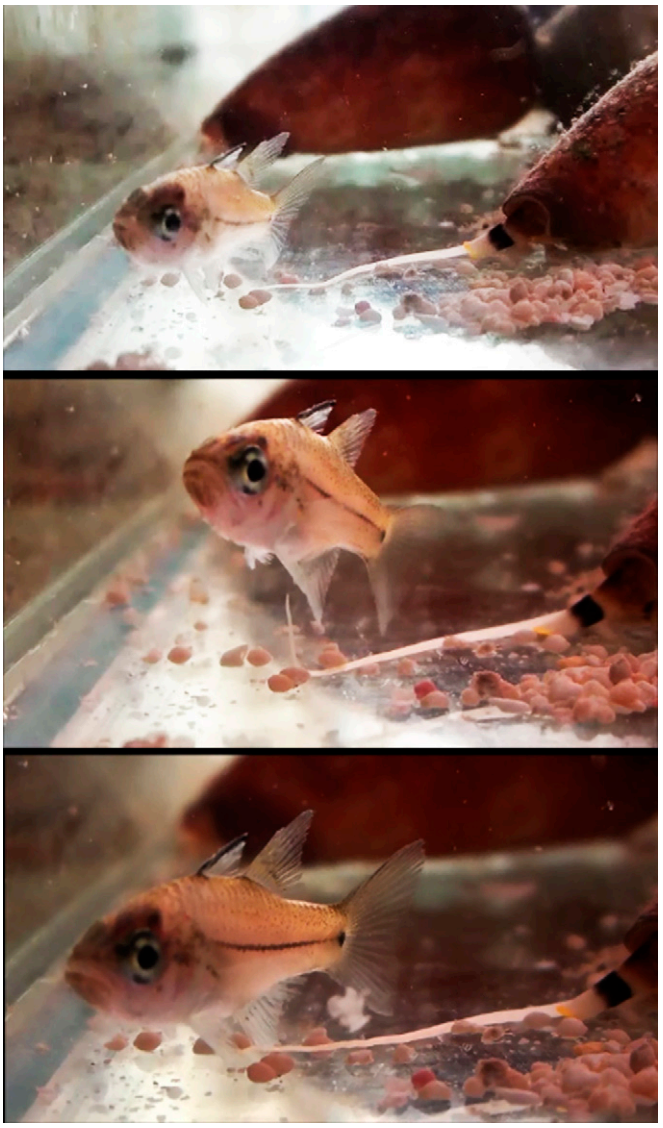

**Movie S2.** *Conus tessulatus* attempting to envenomate a fish. The snail extends its proboscis towards the fish, but when it contacts the fish fin, it apparently ejects a radular tooth and a cloud of venom is released. This records an unsuccessful attempt by *Conus tessulatus* to prey on fish (still photos from this video are included in Fig. 5).

Movie S2